π-Acid Ligands in Iron(III) Porphyrinates. Characterization of Low-Spin Bis(*tert*-butylisocyanide)(porphyrinato)iron(III) Complexes Having $(d_{xz},d_{yz})^4(d_{xy})^1$ Ground States

F. Ann Walker,*,† Habib Nasri,‡,§ Ilona Turowska-Tyrk,‡,⊥ K. Mohanrao,‡ C. Todd Watson,† Nikolai V. Shokhirev,†,∥ Peter G. Debrunner,*,£ and W. Robert Scheidt*,‡

Contribution from the Department of Chemistry, University of Arizona, Tucson, Arizona 85721, Department of Chemistry and Biochemistry, University of Notre Dame, Notre Dame, Indiana 46556, and Department of Physics, University of Illinois, Urbana-Champaign, Illinois 61801

Received June 11, 1996[⊗]

Abstract: The synthesis and characterization of isocyanide complexes of (porphyrinato)iron(III) species, [(Porph)Fe(*t*-BuNC)$_2$]ClO$_4$, Porph = OEP, TPP, are reported. The crystal structures of [(TPP)Fe(*t*-BuNC)$_2$]ClO$_4$ and [(OEP)Fe(*t*-BuNC)$_2$]ClO$_4$ have been determined. Consistent with the expected effect from the strong π-acceptor character of the axial *tert*-butyl isocyanide ligands, the X-ray structure of the complex shows that the porphyrinate ring is strongly ruffled. The spectroscopic properties of these complexes suggest the possibility of "blurring" of the definitions of the electron configurations of low-spin Fe(III) macrocycles having $(d_{xy})^1$ electronic ground states, with the extreme possibilities being low-spin Fe(III)-(macrocycle)$^{2-}$, with the unpaired electron localized in the d_{xy} orbital of the metal, and low-spin Fe(II)-(macrocycle)$^{1-\bullet}$, with the unpaired electron localized on the macrocycle. EPR spectroscopy of the TPP and OEP complexes shows that the *g*-values ($g_\perp = 2.20-2.28$, $g_\parallel = 1.94-1.83$) are consistent with an electron configuration that is $(d_{xz},d_{yz})^4(d_{xy})^1$, the purest $(d_{xy})^1$ ground state system with the most complete quenching of orbital angular momentum discovered thus far ($\sum g^2$ as small as 13.5). Proton NMR spectra of [OEPFe(*t*-BuNC)$_2$]ClO$_4$ in CD_2Cl_2, recorded over the temperature range −100 to +37 °C, also support the $(d_{xy})^1$ ground state, where ruffling of the porphyrinate ring makes it possible for unpaired electron spin delocalization to the $3a_{2u}(\pi)$ orbital of the porphyrinate ring. This orbital has very large electron density coefficients at the *meso* positions and hence explains the very large negative contact shift of the *meso*-H; its size indicates considerable (~19%) spin delocalization from low-spin Fe(III) to the $3a_{2u}(\pi)$ orbital by porphyrin → Fe π donation. Mössbauer and IR spectral data are also consistent with the $(d_{xy})^1$ ground state.

Introduction

There have been several recent investigations of the effect of the relative orientations of planar axial ligands,[1−13] and π-acceptor properties of axial ligands,[13−15] on the structural and spectroscopic properties of Fe(III) porphyrinates.[16] Investigation of the molecular structures, EPR spectra, and in some cases Mössbauer spectra of well-defined low-spin heme model compounds with high-basicity pyridines, imidazoles or cyanides as the axial ligands has provided conclusive proof that the "large g_{max}" EPR signal is correlated with near-degeneracy of d_{xz} and d_{yz}.[3,11] For complexes with planar axial ligands, this correlates with perpendicular alignment of these ligands,[3,5,6] while rhombic EPR signals are correlated with parallel alignment of planar axial ligands. On the basis of Griffith's theory[17] and Taylor's formulation[18] the relative energies of the d_{xy}, d_{xz}, and d_{yz} orbitals can be calculated from the *g*-values. In some cases two of the *g*-values must be measured by single crystal EPR spectroscopy[9−11] or estimated from Mössbauer spectra at 4.2 K in the presence

† University of Arizona.
‡ University of Notre Dame.
§ Present address: Faculté des Sciences, Techniques de Monastir, Monsastir 5000, Tunisa.
⊥ Present address: Department of Chemistry, University of Wrocław, 14 F. Joliot-Curie, 50-383 Wrocław, Poland.
∥ On leave from the Institute of Chemical Kinetics and Combustion, USSR Academy of Sciences, Novosibirsk.
£ University of Illinois.
⊗ Abstract published in *Advance ACS Abstracts,* November 15, 1996.

(1) Scheidt, W. R.; Osvath, S. R.; Lee, Y. J. *J. Am. Chem. Soc.* **1987**, *109*, 1958.
(2) Scheidt, W. R.; Kirner, J. F.; Hoard, J. L.; Reed, C. A. *J. Am. Chem. Soc.* **1987**, *109*, 1963.
(3) Walker, F. A.; Huynh, B. H.; Scheidt, W. R.; Osvath, S. R. *J. Am. Chem. Soc.* **1986**, *108*, 5288.
(4) Scheidt, W. R.; Kirner, J. L.; Hoard, J. L.; Reed, C. A. *J. Am. Chem. Soc.* **1987**, *109*, 1963.
(5) Hatano, K.; Safo, M. K.; Walker, F. A.; Scheidt, W. R. *Inorg. Chem.* **1991**, *30*, 1643.
(6) Safo, M. K.; Gupta, G. P.; Walker, F. A.; Scheidt, W. R. *J. Am. Chem. Soc.* **1991**, *113*, 5497.
(7) Safo, M. K.; Gupta, G. P.; Watson, C. T.; Simonis, U.; Walker, F. A. ; Scheidt, W. R. *J. Am. Chem. Soc.* **1992**, *114*, 7066.
(8) Scheidt, W. R.; Chipman, D. M. *J. Am. Chem. Soc.* **1986**, *108*, 1163.
(9) Quinn, R.; Valentine, J. S.; Byrn, M. P.; Strouse, C. E. *J. Am. Chem. Soc.* **1987**, *109*, 3301.
(10) Soltis, S. M.; Strouse, C. E. *J. Am. Chem. Soc.* **1988**, *110*, 2824.
(11) Inniss, D.; Soltis, S. M.; Strouse, C. E. *J. Am. Chem. Soc.* **1988**, *110*, 5644.
(12) Munro, O. Q.; Marques, H. M.; Debrunner, P. G.; Mohanrao, K.; Scheidt, W. R. *J. Am. Chem. Soc.* **1995**, *117*, 935.
(13) Safo, M. K.; Walker, F. A.; Raitsimring, A. M.; Walters, W. P.; Dolata, D. P.; Debrunner, P. G.; Scheidt, W. R. *J. Am. Chem. Soc.* **1994**, *116*, 7760.
(14) Simonneaux, G.; Hindre, F.; Le Plouzennec, M. *Inorg. Chem.* **1989**, *28*, 823.
(15) Cheesman, M. R.; Walker, F. A. *J. Am. Chem. Soc.* **1996**, *118*, 7373.
(16) Abbreviations used include *t*-BuNC, *tert*-butylisonitrile; 4-CNPy, 4-cyanopyridine; *N*-MeIm, N-methylimidazole; 2-MeImH, 2−methylimidazole; OEP, dianion of octaethylporphyrin; TPP, dianion of *meso*-tetraphenylporphyrin; TMP, dianion of *meso*-tetramesitylporphyrin; OEiBC, dianion of octaethylisobacteriochlorin; N_P porphinato nitrogen atom; N_{ax}, axial ligand nitrogen.
(17) Griffith, J. S. *Proc. Roy. Soc. London, A* **1956**, *235*, 23.
(18) Taylor, C. P. S. *Biochim. Biophys. Acta* **1977**, *491*, 137.

S0002-7863(96)01971-3 CCC: $12.00

of an applied magnetic field.[3,6] The results confirm that the parallel orientation is more stable and that perpendicular alignment of planar axial ligands could lead to a positive shift in reduction potential of up to ~50 mV over that observed for parallel alignment, all other structural and environmental factors being equal.[3] These high-basicity pyridine and imidazole complexes of iron(III) porphyrinates have been shown to be good models of the bis-histidine-coordinated cytochromes *b* and *c* that are involved in electron transfer in a large number of organisms, including cytochromes b_5[19] and c_3[20] as well as the membrane-bound cytochromes *b* with probable bis(histidine) coordination,[21] including the two *b* cytochromes of mitochondrial "Complex III" (also known as ubiquinone-cytochrome *c* oxidoreductase) and chloroplast cytochrome b_6.

For some years it was common practice to assign the largest *g*-value to the direction of the heme normal, on the basis of single crystal EPR data for cytochrome c[22] and several model hemes.[9−11] On the basis of Griffith's theory[17] and Taylor's formulation,[18] this assignment was consistent with the major contributor to the orbital of the unpaired electron being d_{yz}. However, Taylor showed that this sometimes leads, as in the systems described herein, to larger calculated energy separations between d_{xz} and d_{yz} (V/λ) than between their average and the lowest-energy d_{xz} orbital (Δ/λ), a situation that he described as an "improper axis system".[18] In such cases, he suggested, by permutation of the assignment of *g*-values one could arrive at calculated ligand field energy differences that obeyed the expected relationship $V/\Delta < {}^2/_3$. This permutation typically led to a change in the major contributor to the orbital of the unpaired electron being d_{xy}, thus placing d_{xy} higher in energy than d_{xz} and d_{yz}. Examples of systems for which this permutation of the assignment of *g*-values was found to be necessary included the bis(imidazole) complex of octaethylchlorinatoiron(III).[18] There are, however, a number of definite cases in which V/Δ is $> {}^2/_3$, yet the unpaired electron is in d_{yz} orbital.[23] However, as we will show below, the complexes of the current study do *not* violate Taylor's formulation.

In our recent determinations of the structures of a series of $[(TMP)Fe(L)_2]ClO_4$ complexes in which L is a pyridine (4-NMe_2Py,[6] 3-EtPy,[7] 3-ClPy,[7] 4-CNPy,[7] and 3-CNPy[7]) or imidazole (N-MeIm[6] or 2-MeImH[12]) we have shown that, as expected from their large g_{max} EPR spectra,[6,7] both pyridine and hindered imidazole ligands are aligned in perpendicular planes. In the complexes of low-basicity pyridines, we noted both large variations and unusually small EPR *g*-values and Mössbauer quadrupole splittings.[7] We suggested that the large range and especially the unusually small ΔE_Q and *g*-values were related to the axial ligand π-bonding properties, which led to significant changes in the relative energies of the d_{xy}, d_{xz}, and d_{yz} orbitals.[7] Indeed, with very strong π-accepting ligands, such as 3- and 4−cyanopyridines, the orbital energies appear to have changed so markedly that the d_{xy} orbital is *higher* in energy than the d_{xz},d_{yz} pair.[7] In other words, there are two quite distinct, limiting ground states for low-spin iron(III) in this series of iron(III) porphyrinates: (a) the generally observed $(d_{xy})^2(d_{xz},d_{yz})^3$ state and (b) the novel $(d_{xz},d_{yz})^4(d_{xy})^1$ state where the d_{xz},d_{yz} pair are degenerate, or nearly so, and *below* the d_{xy} orbital in energy. For symmetrical porphyrinate rings, this latter electronic state leads to an *axial* EPR spectrum, with $g_\perp > g_{||}$,[7] rather than the usual rhombic or large g_{max} EPR signal.[3,6] We then showed, in a study of the "nonhindered" tetraphenylporphyrinate complex $[(TPP)Fe(4\text{-}CNPy)_2]ClO_4$,[13] that for axial ligands that have strong π-acceptor properties there is an *electronic* stabilization of the $(d_{xz},d_{yz})^4(d_{xy})^1$ electronic ground state. The strong ruffling observed for the tetramesitylporphyrinate complexes was maintained for this (TPP)Fe(III) complex and led us to postulate that the $(d_{xy})^1$ electronic ground state could be stabilized by π electron donation from the $3a_{2u}(\pi)$ orbital of the porphyrinate ring. Such electron donation becomes symmetry-allowed when the $p_z(\pi)$ orbitals of the porphyrinate nitrogens are twisted from the normal to the mean plane of the porphyrinate ring.[13]

We then studied the MCD spectra of $[(TMP)Fe(4\text{-}CNPy)_2]ClO_4$ and showed that they bear a strong resemblence to those of low-spin iron(III) chlorins, especially in terms of the low intensities of the MCD bands in both the visible and near IR regions of the electronic spectra.[15] Not only the low-intensity visible[24] and near IR[25] MCD bands but also the EPR *g*-values of iron chlorins[18,26−30] and proteins that contain them[30,31] are very similar to those of $[(TMP)Fe(4\text{-}CNPy)_2]ClO_4$.[13] Thus, it is now apparent that iron(III) tetraphenyl*porphyrinates*, when bound to low-basicity, strong π-acceptor ligands, are good models of the "green hemes" that include *(i)* the iron chlorin that is the prosthetic group of hydroperoxidase II[32a] and cytochrome *bd*[32b] from *Escherichia coli* and *(ii)* the iron dioxoisobacteriochlorin of heme d_1, the prosthetic group of the dissimilatory nitrite reductases of denitrifying bacteria[33] as well as *(iii)* the siroheme prosthetic group of bacterial sulfite and nitrite reductases.[34]

The unusual EPR and Mössbauer parameters of the low-basicity pyridine iron tetramesitylporphyrinate complexes are fully reflected in their ^{1}H NMR spectra; at −80 °C the pyrrole-H isotropic shifts varies smoothly from −40 ppm (L = 4-NMe_2-Py) to −6 ppm (L = 4-CNPy) as the basicity of the pyridine ligand decreases.[7] Earlier ^{1}H NMR investigations of the related $[(TPP)Fe(L)_2]^+$ complexes by La Mar and co-workers[35] had shown a similar but less pronounced trend in the pyrrole-H isotropic shifts as a function of pyridine basicity. Thus, whereas it has been accepted that low-spin Fe(III) porphyrinates bound to basic pyridines, imidazoles, and cyanide have a $(d_{xy})^2(d_{xz},d_{yz})^3$ ground state that gives rise to rhombic EPR spectra and ^{1}H NMR spin delocalization to protons on the periphery of the molecule *via* the filled 3e(π) porphyrin orbitals, *i.e.*, P → Fe π bond-

(19) Mathews, F. S.; Czerwinski, E. W.; Argos, P. in *The Porphyrins*; Dolphin, D., Ed.; Academic Press: New York, 1979; Vol. VII; p 108.
(20) Pierrot, M.; Haser, R.; Frey, M.; Payan, F.; Astier, J.-P. *J. Biol. Chem.* **1982**, *257*, 14341. Higuchi, Y.; Kusunoki, M.; Matsuura, Y.; Yasuoka, N.; Kakudo, M. *J. Mol. Biol.* **1984**, *172*, 109.
(21) Widger, W. R.; Cramer, W. A.; Herrmann, R. G.; Trebst, A. *Proc. Natl. Acad. Sci. USA* **1984**, *81*, 674. Babcock, G. T.; Widger, W. R.; Cramer, W. A.; Oertling, W. A.; Metz, J. *Biochemistry* **1985**, *24*, 3638.
(22) Mailer, C.; Taylor, C. P. S. *Can. J. Biochem.* **1972**, *50*, 1048.
(23) Raitsimring, A. M.; Borbat, P.; Shokhireva, T. Kh.; Walker, F. A. *J. Phys. Chem.* **1996**, *100*, 5235; Nasri, H.; Wang, Y.; Huynh, B. H.; Walker, F. A.; Scheidt, W. R. *Inorg. Chem.* **1991**, *30*, 1483; Devaney, P. W., Ph.D. Thesis, University of Illinois, 1980.
(24) Bracete, A. M.; Kadkhodayan, S.; Sono, M.; Huff, A. M.; Zhuang, C.; Cooper, D. K.; Smith, K. M.; Chang, C. K.; Dawson, J. H. *Inorg. Chem.* **1994**, *33*, 5042.
(25) (a) Peng, Q.; Timkovich, R.; Loewen, P. C.; Peterson, J. *FEBS Lett.* **1992**, *309*, 157. (b) Peng, Q.; Peterson, J. *FEBS Lett.* **1994**, *356*, 159.
(26) Gudat, J. C.; Singh, J.; Wharton, D. C. *Biochim. Biophys. Acta* **1973**, *292*, 376.
(27) Stolzenberg, A. M.; Strauss, S. H.; Holm, R. H. *J. Am. Chem. Soc.* **1981**, *103*, 4763.
(28) Muhoberac, B. B.; Wharton, D. C. *J. Biol. Chem.* **1983**, *258*, 3019.
(29) Muhoberac, B. B. *Arch. Biochem. Biophys.* **1984**, *233*, 682.
(30) Coulter, E. D.; Sono, M.; Chang, C. K.; Lopez, O.; Dawson, J. H. *Inorg. Chim. Acta* **1995**, *240*, 603.
(31) Sutherland, J.; Greenwood, C.; Peterson, J.; Thomson, A. J. *Biochem. J.* **1986**, *233*, 893.
(32) (a) Chiu, J. T.; Loewen, P. C.; Switala, J.; Gennis, R. B.; Timkovich, R. *J. Am. Chem. Soc.* **1989**, *111*, 7046. (b) Lorence, R. M.; Gennis, R. B. *J. Biol. Chem.* **1989**, *264*, 7135.
(33) Chang, C. K.; Wu, W. *J. Biol. Chem.* **1986**, *261*, 8593.
(34) Crane, B. R.; Siegel, L. M.; Getzoff, E. D. *Science* **1995**, *270*, 59.
(35) La Mar, G. N.; Bold, T. J.; Satterlee, J. D. *Biochim. Biophys. Acta* **1977**, *498*, 189.

ing,[36,37] it has recently been recognized[7,13,14] that with certain kinds of axial ligands (isocyanides,[14] low-basicity pyridines[7,35]) or certain modifications of the porphyrin π orbitals (such as occurs in the reduced hemes), the $(d_{xz},d_{yz})^4(d_{xy})^1$ electron configuration is stabilized and leads to ^{1}H NMR spectra that show just the reverse types of π spin delocalization patterns: negligible π spin delocalization to the β-pyrrole positions but large π spin delocalization to the *meso* positions.[7,37] In this case, although the d_{xz},d_{yz} orbital set, which has proper symmetry for π spin delocalization, is filled, the d_{xy} orbital can acquire proper symmetry for overlap with the $a_{2u}(\pi)$ orbital of the porphyrin ring[38−40] if the porphyrin ring is highly ruffled.[13]

The most extreme example of this latter behavior of the ^{1}H NMR spectra of low-spin Fe(III) porphyrinate complexes with π-acceptor ligands reported to date is that of the bis-isocyanide complex, initially reported by Simonneaux and co-workers for $[(TPP)Fe(t\text{-BuNC})_2]^+$,[14] for which the pyrrole-H shift is very close to that expected for a *diamagnetic* porphyrin.[41] Following this interesting report we investigated the EPR spectrum of this complex and found that the spectrum was axial with $g_\perp \sim 2.2$ and $g_\parallel \sim 1.9$, leading to a value of $\sum g^2$ of ~13.5. This extremely small value suggested that the $(d_{xy})^1$ ground state of these complexes was much more "pure" than that of the bis-4-cyanopyridine complexes, such that there was extreme quenching of the orbital angular momentum of the unpaired d electron. We then began investigating the isocyanide complexes of other Fe(III) porphyrinates and found similar EPR spectra, whose *g*-values are somewhat reminiscent of those of the bis-(isocyanide) complex of Fe(III) octaethylisobacteriochlorinate, $[(OEiBC)Fe(RNC)_2]^+$, which has been formulated as the internal electron transfer form, Fe(II)(OEiBC cation radical).[42] While the values of $g_\perp$ and $g_\parallel$ are both *closer* to 2.0 in this case,[42] one of the questions raised by the present work is whether the unpaired electron in the isobacteriochlorin case is indeed located on the iron rather than the macrocycle, or, from another point of view, whether there is a blurring of the definitions of whether the electron is metal-based or macrocycle-based, or again, whether there is a facile "internal redox" possible between the metal and macrocyclic ligand that means that both forms are populated to some extent. This question has important implications for the rates of electron transfer and the nature of enzymatic reactions of the so-called green hemes.

In this paper we report the crystal and molecular structure of $[(TPP)Fe(t\text{-BuNC})_2]ClO_4$ and $[(OEP)Fe(t\text{-BuNC})_2]ClO_4$, the IR, EPR, and Mössbauer spectra of these complexes, and a detailed study of the ^{1}H NMR spectrum of $[(OEP)Fe(t\text{-BuNC})_2]^+$ in deuterodichloromethane over most of its liquid range. On the basis of the structural and spectroscopic data obtained, we conclude that these are the purest examples of the $(d_{xz}d_{yz})^4(d_{xy})^1$ electronic ground state reported thus far and that the extreme ruffling of the porphyrinate ring facilitates extensive delocalization of the d_{xy} unpaired electron into the porphyrinate $3a_{2u}(\pi)$ orbital. These findings have important implications for the interpretation of the NMR spectra of low-spin Fe(III) complexes of the reduced heme macrocycles.

Experimental Section

General Information. All reactions were carried out under argon in Schlenkware. All solvents were distilled under argon prior to use. Chloroform, chlorobenzene, and hexane were distilled over calcium hydride and toluene was distilled from sodium benzophenone ketyl. *tert*-Butyl isocyanide was obtained from Aldrich and used without further purification. H_2TPP[43] was synthesized while H_2OEP was obtained from Midcentury Chemicals and used without further purification. $^{57}Fe_2O_3$ was obtained from New England Nuclear. Perchlorato(porphyrinato)iron(III) derivatives were prepared by modification of reported procedures.[44] EPR spectra were obtained at 77 K with a Varian E-Line EPR spectrometer operating at X-band frequency. Liquid helium EPR spectra were recorded on a Bruker ESP-300E EPR spectrometer operating at X-band and equipped with an Oxford helium cryostat. Spectra were obtained for samples in frozen CH_2Cl_2 solution and as polycrystalline solids. UV-visible spectra were recorded on a Perkin-Elmer Lambda 19 spectrometer, and IR spectra were recorded on a Perkin-Elmer Lambda 883 spectrometer as KBr pellets. Mössbauer spectra were recorded at various temperatures and magnetic fields on constant-acceleration spectrometers. Several preparations of the compounds were studied to assess their homogeneity, and the samples were obtained from ground single crystals in apiezon or as frozen chlorobenzene solutions. The data were analyzed in terms of a spin Hamiltonian model in the limit of slow or fast spin fluctuation rates,[45] respectively. Isomer shifts are quoted relative to iron metal at room temperature. Proton NMR spectra were recorded on a Bruker AM250 NMR spectrometer. Samples (10 mM) were prepared in CD_2Cl_2 (Cambridge) and recorded at temperatures ranging from −100 to +37 °C. The temperature controller was calibrated using the standard methanol and ethylene glycol VT samples (Wilmad) using the standard calibration curve.

Synthesis of $[(OEP)Fe(t\text{-BuNC})_2]ClO_4$. $[(OEP)Fe(OClO_3)]$ (60 mg, 0.087 mmol) was dissolved in chloroform (7 mL) in a Schlenk flask and approximately 0.5 mL of *tert*-butyl isocyanide was added. The solution immediately changed to a cherry red color. The reaction mixture was stirred for 5 min, and 5 mL of toluene was added. Hexane was then layered for crystallization. After 5 days, crystals were harvested. UV-vis ($CHCl_3$, excess *tert*-butyl isocyanide): λ_{max}, nm (log ϵ): 405 (4.90) Soret, 535 (4.02), 559 (4.02), 685 (3.02). IR (KBr pellet), ν(NC), 2193 cm^{-1}. EPR (CH_2Cl_2 glass, 77 K): $g_\perp = 2.28$, $g_\parallel = 1.83$.

Synthesis of $[(TPP)Fe(t\text{-BuNC})_2]ClO_4$. This compound was prepared and crystallized as above using either chloroform or chlorobenzene as solvent. UV-vis ($CHCl_3$, excess *tert*-butyl isocyanide): λ_{max}, nm (log ϵ): 420 (5.03) Soret, 531 (3.99), 715 (2.92), 764 (2.86). IR (KBr pellet), ν(NC), 2200 cm^{-1}. EPR (CH_2Cl_2 glass, 77 K): $g_\perp = 2.21$, $g_\parallel = 1.93$.

Synthesis of $[(TPP)^{57}Fe(t\text{-BuNC})_2]ClO_4$. $[(TPP)^{57}FeCl]$ (60 mg, 0.085 mmol, 57% enriched) was synthesized as described,[46] dissolved in CH_2Cl_2 (50 mL), and washed with two 50-mL portions of 2 M KOH and then with water. The resulting μ-oxo complex was converted to the perchlorato complex by washing with two 50-mL portions of 60% $HClO_4$ and then with 10% $HClO_4$. The organic layer was dried over anhydrous magnesium sulfate and concentrated to 10 mL, and dry pentane was added. $[(TPP)^{57}Fe(OClO_3)]$ was precipitated. The precipitate was washed twice with pentane and dried (yield 60 mg). A 4 mg (0.006 mmol) portion of this complex was dissolved in 0.3 mL of chlorobenzene in a nylon Mössbauer sample holder, and an excess

(36) La Mar, G. N.; Walker, F. A. in *The Porphyrins*; Dolphin, D., Ed.; Academic Press: New York, 1979; Vol. IVB; pp 57−161.

(37) Walker, F. A.; Simonis, U. In *Biological Magnetic Resonance, Volume 12: NMR of Paramagnetic Molecules*; Berliner, L. J.; Reuben, J., Eds.; Plenum Press: New York, 1993; pp 133−274.

(38) It must be noted that since the temperatures at which EPR and NMR spectra are recorded, 4−77 K *vs* ~190−340 K, respectively, there is not necessarily a direct correspondence between the electron configuration observed by EPR spectroscopy and that observed by NMR spectroscopy.[37] This appears to be particularly true of the low-spin Fe(III) complexes of the reduced hemes.[39,40]

(39) Keating, K. A.; La Mar, G. N.; Shiau, F.-Y.; Smith, K. M. *J. Am. Chem. Soc.* **1992**, *114*, 6513.

(40) Licoccia, S.; Chatfield, M. J.; La Mar, G. N.; Smith, K. M.; Mansfield, K. E.; Anderson, R. R. *J. Am. Chem. Soc.* **1989**, *111*, 6087.

(41) More recently Simonneaux and co-workers have reported two additional ligands that appear to yield $(d_{xz},d_{yz})^4(d_{xy})^1$ states: trifluoroethylisocyanide (Gèze, C.; Legrand, N.; Bondon, A.; Simonneaux, G. *Inorg. Chim. Acta* **1992**, *195*, 73) and phosphonites (Guillemot, M.; Simonneaux, G. *J. Chem. Soc., Chem. Commun.* **1995**, 2093).

(42) Sullivan, E. P.; Strauss, S. H. *Inorg. Chem.* **1989**, *28*, 3093.

(43) Adler, A. D.; Longo, F. R.; Finarelli, J. D.; Goldmacher, J.; Assour, J.; Korsakoff, T. *J. Org. Chem.* **1967**, *32*, 476.

(44) Dolphin, D. H.; Sams, J. R.; Tsin, T. B. *Inorg. Chem.* **1977**, *16*, 711.

(45) Münck, E.; Groves, J. L.; Tumolillo, T. A.; Debrunner, P. G. *Computer Phys. Commun.* 1973.

(46) Landergren, M.; Baltzer, L. *Inorg. Chem.* **1990**, *29*, 556.

Table 1. Crystallographic Data for [(TPP)Fe(*t*-BuNC)2]ClO_4 and [(OEP)Fe(*t*-BuNC)$_2$]ClO_4

molecule	[(TPP)Fe(*t*-BuNC)$_2$]ClO_4·$(C_6H_5Cl)_{0.75}$	[(OEP)Fe(*t*-BuNC)$_2$]ClO_4
formula	$C_{54}H_{41}ClFeN_6O_4$·$(C_6H_5Cl)_{0.75}$	$C_{46}H_{62}ClFeN_6O_4$
FW, amu	1013.68	854.34
a, Å	10.507 (13)	9.756 (6)
b, Å	13.494 (38)	15.065 (8)
c, Å	37.158 (98)	17.753 (8)
α, deg	90.0	67.38 (5)
β, deg	92.63 (22)	82.29 (4)
γ, deg	90.0	74.43 (4)
V, Å^3	5263 (36)	2318.5(8)
space group	$P2_1/c$	$P\bar{1}$
crystal system	monoclinic	triclinic
Z	4	2
μ, mm^{-1}	0.418	0.427
temp, K	293 (1)	293 (1)
R_1	0.104	0.052
R_2	0.116	0.073

(2 drops) of *tert*-butyl isocyanide was added, sealed, frozen, and used for solution Mössbauer measurements.

Structure Determinations.[47] A suitable dark purple crystal of [(OEP)Fe(*t*-BuNC)$_2$]ClO_4 was examined with graphite-monochromated Mo Kα radiation on an Enraf-Nonius CAD4 diffractometer at 293 K. Precise values of unit cell parameters were determined by least-squares treatment of setting angles of 25 reflections. Final cell constants are reported in Table 1. Profiles of a total of 9545 reflections with $2\Theta \leq 54.9°$ were measured using the $\omega-2\Theta$ scan technique. Four standard reflections were monitored during data collection, and no significant decay was observed. The intensity data were reduced using the Blessing[48] data reduction programs with corrections for Lorentz and polarization effects. A total of 6716 reflections with $F_o \geq 3.0\sigma(F_o)$ were considered as observed and used in all subsequent calculations. The structure was solved by direct methods using MULTAN.[49] The positions of 46 non-hydrogen atoms were found. The remaining atoms were found in difference Fourier maps. For all non-hydrogen atoms, anisotropic full-matrix least squares refinement was used. Hydrogen atoms (whose locations were suggested by difference Fourier) were included in subsequent cycles of least-squares refinement as fixed, idealized contributors (C−H = 0.95 Å, B(H) = 1.3 × B(C) Å^2). The maximum electron density on the final difference Fourier map was 0.49 e/Å^3 at 0.97 Å from the Fe atom and the minimum was 0.42 e/Å^3. The final refinement converged to a conventional $R_1 = 0.052$ and $R_2 = 0.073$ and goodness of fit was $S = 2.17$. Final atomic coordinates are listed in Table S8.

A crystal of [(TPP)Fe(*t*-BuNC)$_2$]ClO_4·0.75(C_6H_5Cl) was examined with graphite monochromated Mo Kα radiation on an Enraf-Nonius FAST area detector diffractometer at 293 K. Unit cell parameters were determined from 250 reflections collected for three rotations, separated by 45°. Data collection procedures with an area detector are described elsewhere;[50] a summary is given in Table S1. Intensities of all reflections were reduced using Lorentz and polarization corrections. A total of 4551 reflections were considered as observed ($F_o \geq 1.9\sigma(F_o)$), of which 2664 were unique. The structure was solved by Patterson methods from the SHELXS86 program.[49] Positions of most atoms were revealed. Several atoms from a phenyl ring and a perchlorate anion and all from a chlorobenzene molecule were found in subsequent difference Fourier maps. Anisotropic full-matrix least-squares refinement was used for all non-hydrogen atoms. Hydrogen atoms were included as fixed, idealized contributors. The refinement converged to a final value of $R = 0.104$ and $wR_2 = 0.116$. The maximum and minimum electron density on the final difference Fourier map was 0.62 and −0.68 e/Å^3, respectively. Final atomic coordinates are listed in Table S2.

Results and Discussion

Structures of the Bis(isocyanide) Complexes. The complexes [(TPP)Fe(*t*-BuNC)$_2$]ClO_4 and [(OEP)Fe(*t*-BuNC)$_2$]ClO_4 have been characterized by UV-vis, IR, EPR, Mössbauer, and single-crystal X-ray structure determinations. [(TPP)Fe(*t*-BuNC)$_2$]$^+$ has previously been characterized by ^{1}H NMR spectroscopy,[14] and [(OEP)Fe(*t*-BuNC)$_2$]ClO_4 has been similarly characterized in the present work. The molecular structure of [(TPP)Fe(*t*-BuNC)$_2$]ClO_4 is displayed in Figure 1 which also shows the numbering scheme for the atoms. Averaged values[51] for the chemically equivalent bond distances and angles are shown in Figure 2; complete distance and angle tabulations are given in the Supporting Information. The average values for the distances and angles within the porphyrin core are not remarkable. However, the average Fe−N_P bond distances of 1.951(23) Å is quite short for a low-spin iron(III) porphyrinate. A second noteworthy and important feature is the core conformation. Figure 2 displays the values of the perpendicular displacements, in units of 0.01 Å, from the mean plane of the 24-atom porphyrin core. The strong D_{2d}-ruffling of the core is quite apparent. Indeed, this compound is among the most strongly ruffled iron(III) derivatives yet characterized. As pointed out by Hoard,[52] core ruffling and short M−N_P bonds are tightly coupled parameters, with core ruffling leading to shortened M−N_P bonds. In general, it has been presumed that the coordination requirements of the metal ion leading to short M−N_P bonds predominate and ruffled cores thus ensue.

The shortest Fe−N_P distance for a low-spin iron(III) complex is the 1.937(12) Å-value found for [(TMP)Fe(2-MeImH)$_2$]ClO_4;[12] this species also has a strongly ruffled porphyrinato core. For this complex, the origin of the strong ruffling and the concomitant short Fe−N_P bond distances are the steric interactions between the porphyrin core and the bulky axial 2−methylimidazole ligands, which are found in orthogonal planes. The

(47) An initial structure determination for [(TPP)Fe(*t*-BuNC)$_2$]ClO_4 was undertaken, but not completed. The cell was similar to the one reported here (the *c*-axis was approximately 2 Å longer and contained additional solvent). All structural results were essentially the same as for the derivative reported herein. Nasri, H.; Haller, K. J.; Scheidt, W. R., unpublished.

(48) Blessing, R. H. *Cryst. Rev.* **1987**, *1*, 3.

(49) Programs used in this study included SHELXS86 (Sheldrick, G. M. *Acta Crystallogr., Sect. A* **1990**, *A46*, 467), local modifications of Main, Hull, Lessinger, Germain, Declerq, and Woolfson's MULTAN, Jacobson's ALLS, Zalkin's FORDAP, Busing and Levy's ORFFE and ORFLS, and Johnson's ORTEP2. Atomic form factors were from Cromer, D. T.; Mann, J. B. *Acta Crystallogr., Sect. A* **1968**, *A24*, 321. Real and imaginary corrections for anomalous dispersion in the form factor of the iron atom was from Cromer, D. T.; Liberman, D. J. *J. Chem. Phys.* **1970**, *53*, 1891. Scattering factors for hydrogen were from Stewart, R. F.; Davidson, E. R.; Simpson, W. T. *J. Chem. Phys.* **1965**, *42*, 3175.

(50) Scheidt, W. R.; Turowska-Tyrk, I. *Inorg. Chem.* **1994**, *33*, 1314.

(51) The numbers in parentheses for this and other averages represent an esd calculated on the assumption that all averaged values are drawn from the same population. The relatively large value seen in the TPP derivative but not the OEP derivative reflect the lower precision obtained for the TPP structure. Nonetheless, there is good internal consistency between the two derivatives.

(52) Hoard, J. L. *Ann. N. Y. Acad. Sci.* **1973**, *206*, 18.

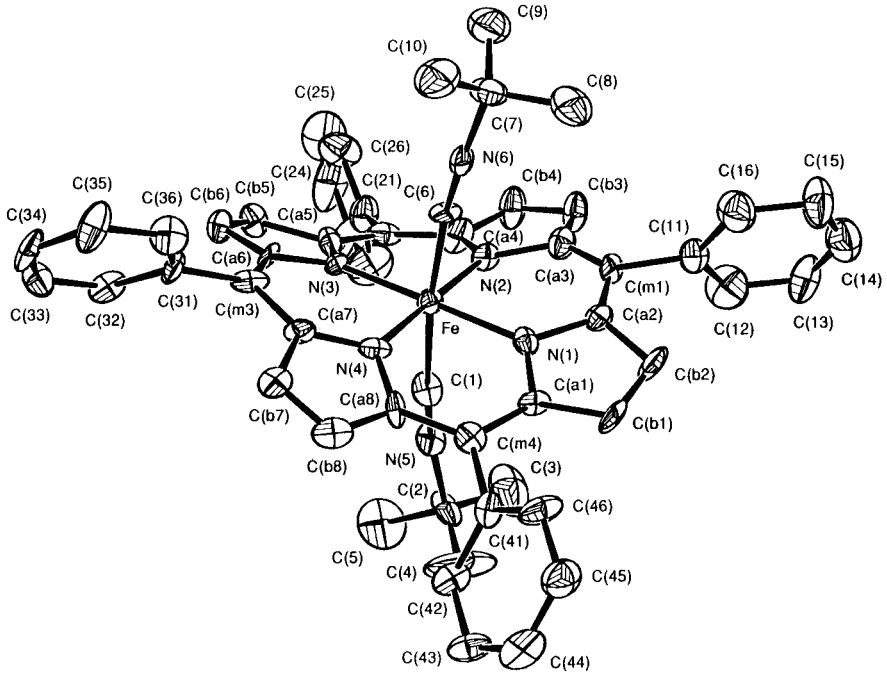

Figure 1. ORTEP diagram for $[(TPP)Fe(t\text{-}BuNC)_2]^+$. Ellipsoids are drawn at the 50% probability level. Atomic labels are displayed.

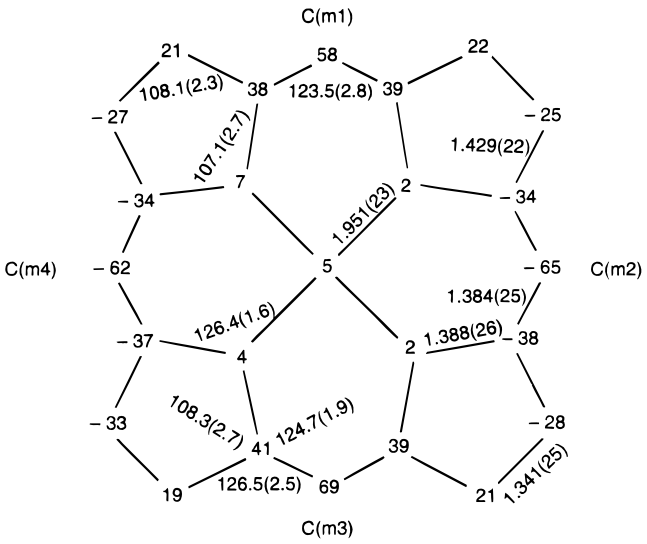

Figure 2. Formal diagram of $[(TPP)Fe(t\text{-}BuNC)_2]^+$ showing the displacements of the atoms, in units of 0.01 Å, from the mean plane of the 24-atom core. Averaged values of bond distances and angles in the porphinato core are also shown.

bulky methyl groups are accommodated by a ruffling of the core with the short Fe−N_P bonds thus following. For $[(TPP)Fe(t\text{-}BuNC)_2]ClO_4$, there are no apparent steric reasons for the observed conformation, which immediately leads to the conclusion that the ruffling and short Fe−N_P distances result from electronic factors.

In order to further test the idea that the ruffled core conformation and the resultant short Fe−N_P bonds in bis(isocyanide)(porphyrinato)iron(III) complexes result from electronic effects, we have determined the molecular structure of the octaethylporphyrin analogue, $[(OEP)Fe(t\text{-}BuNC)_2]ClO_4$. A comparison of otherwise identical TPP and OEP derivatives (with any metal) shows that the OEP derivatives are much more likely to display a planar core even when the precisely analogous TPP derivative shows a substantially ruffled core. Indeed, significantly ruffled cores in OEP derivatives are quite rare, and to our knowledge there are none for iron(III) derivatives.

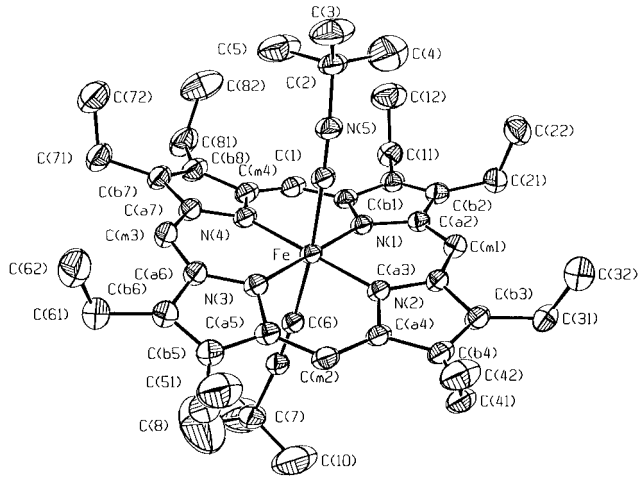

Figure 3. ORTEP diagram for $[(OEP)Fe(t\text{-}BuNC)_2]^+$. Ellipsoids are drawn at the 50% probability level. Atomic labels are displayed.

The molecular structure of $[(OEP)Fe(t\text{-}BuNC)_2]ClO_4$ is displayed in Figure 3 along with the numbering scheme for the atoms. Averaged values for the chemically equivalent bond distances and angles are shown in Figure 4; distances and angles within the porphyrin core are unremarkable. Complete distance and angle tabulations are given in the Supporting Information. A ruffled core and relatively short Fe−N_P distances are again noteworthy features that are clearly seen in the figures. Although the porphinato core is not as ruffled as in the analogous TPP derivative, the magnitude of the ruffling is still substantial. The ruffling also leads to an average Fe−N_P bond distance of 1.9769(13) Å, again quite short but not as short as in the TPP derivative, consistent with the lesser degree of ruffling. We believe that at least part of the variation in ruffling results from differences in the intrinsic core flexibility of the two types of porphyrin ligands.[53] However, the relatively unusual stereochemistry allows us to conclude that these coupled structural features of core ruffling and short Fe−N_P bonds are

(53) Cheng, B.; Munro, O. Q.; Marques, H. M.; Scheidt, W. R. Manuscript to be submitted.

Table 2. Selected Bond Lengths and Distances in $[(TPP)Fe(t\text{-}BuCN)_2]ClO_4$ and $[(OEP)Fe(t\text{-}BuCN)_2]ClO_4$[a]

A. Distances, Å

bond	TPP	OEP	bond	TPP	OEP
Fe−N(1)	1.962 (16)	1.9848 (23)	Fe−C(1)	1.928 (22)	1.929 (3)
Fe−N(2)	1.954 (16)	1.9515 (28)	Fe−C(6)	1.902 (18)	1.925 (3)
Fe−N(3)	1.969 (15)	1.9771 (24)	C(1)−N(5)	1.129 (22)	1.145 (4)
Fe−N(4)	1.918 (16)	1.9944 (28)	C(6)−N(6)	1.117 (20)	1.144 (4)

B. Angles, deg

angle	TPP	OEP	angle	TPP	OEP
N(1)−Fe−N(2)	91.0 (6)	89.95 (10)	C(1)−Fe−N(3)	94.1 (8)	96.94 (11)
N(1)−Fe−N(3)	178.5 (6)	179.55 (10)	C(1)−Fe−N(4)	91.2 (7)	84.25 (12)
N(1)−Fe−N(4)	89.0 (6)	90.08 (11)	C(6)−Fe−N(1)	88.8 (7)	96.10 (11)
N(2)−Fe−N(3)	90.5 (6)	90.43 (11)	C(6)−Fe−N(2)	88.4 (7)	90.91 (12)
N(2)−Fe−N(4)	179.2 (6)	179.34 (9)	C(6)−Fe−N(3)	91.3 (7)	83.66 (12)
N(3)−Fe−N(4)	89.5 (7)	89.55 (11)	C(6)−Fe−N(4)	92.3 (7)	89.74 (12)
C(1)−Fe−N(1)	85.9 (7)	83.26 (11)	C(6)−Fe−C(1)	173.6 (8)	173.96 (12)
C(1)−Fe−N(2)	88.0 (7)	95.09 (12)	Fe−C(1)−N(5)	174.8 (9)	166.34 (26)
			Fe−C(6)−N(6)	173.8 (9)	169.80 (26)

[a] The numbers in parentheses are the estimated standard deviations.

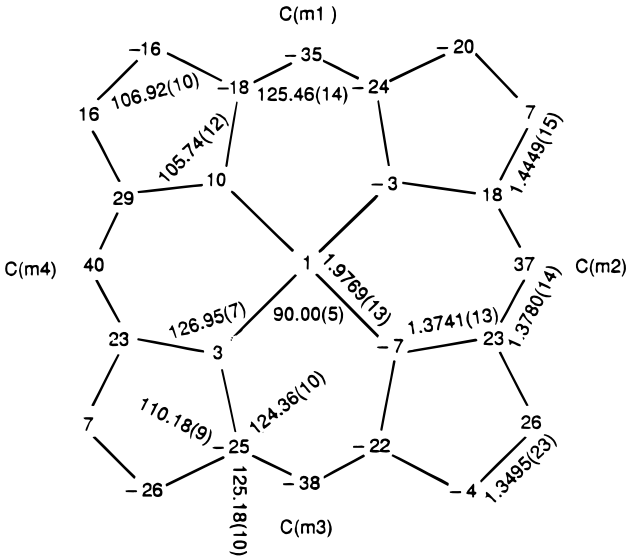

Figure 4. Formal diagram of $[(OEP)Fe(t\text{-}BuNC)_2]^+$ showing the displacements of the atoms, in units of 0.01 Å, from the mean plane of the 24-atom core. Averaged values of bond distances and angles in the porphinato core are also shown.

driven by electronic factors specific to the nature of the axial isocyanide ligands.

Table 2 presents the distances and angles around the iron(III) atom in the two complexes. The lack of ideal geometry around the iron(III) atom in both complexes is immediately evident in the ORTEP diagrams (Figures 1 and 3) and the values in the table. The C−Fe−N_P angles vary between 83−97° and the C−Fe−C angles are decidedly nonlinear (∼174°). The Fe−C−N groups are also not quite linear. A similar lack of ideal geometry around the iron atom was seen in a bis(isocyanide)-iron(II) porphyrinate complex.[54] The average Fe−C distance in the OEP derivative is a short 1.927 (3) Å; the values in the TPP species are similar. These distances are somewhat shorter (1.901(3) Å) in the analogous iron(II) species[54] and are consistent with expected differences in π bonding between a d^5 and a d^6 metal ion. There are also two bis(isocyanide)-(phthalocyanato)iron(II) derivatives;[55,56] each has Fe−C bonds of 1.911 to 1.913 Å. To our knowledge there is only one nominally iron(III) derivative; in this organometallic derivative the Fe−C bond distance is 1.798(10) Å.[57] Collins *et al.*[58] have reported that two isocyanides can be the trans axial ligands to iron in an iron(IV) macrocycle; in this case the Fe−C distances are 1.973 and 1.965 Å. The Fe−C bond lengths can be compared with the Fe−C distances in six-coordinate mono- and bis(cyano)iron(III) derivatives and are similar to slightly longer.[59−62]

Infrared Spectra. The IR spectra of the complexes exhibit ν(NC) stretching frequencies at 2193 and 2200 cm^{-1} (Table 3) compared to 2127 to 2143 cm^{-1} observed for the free ligand.[63] These frequencies are not unusual for metal complexes of isocyanide.

UV-vis Spectra. The UV-vis spectra of the isocyanide derivatives are typical of metalloporphyrin derivatives with neutral porphyrin rings. In particular, they are quite unlike that reported for carbonyl(pyridine)iron(II) tetrabenzporphyrin π-cation radical.[64] This π-cation species has the typical broad, very weak bands in the visible region, quite unlike those of the isocyanide derivatives.

EPR Spectra. The EPR spectra of $[(TPP)Fe(t\text{-}BuNC)_2]ClO_4$ in the polycrystalline solid state and in frozen CH_2Cl_2 solution are shown in Figure 5. As can be seen, the spectra are extremely similar in these two media, with $g_\perp = 2.20$, $g_\parallel = 1.94$ in the solid state and $g_\perp = 2.21$, $g_\parallel = 1.93$ in frozen solution. EPR g-values and crystal field parameters calculated for both complexes are listed in Table 3, along with the coordinated isocyanide N−C stretching frequency, ν(NC). The crystal field parameters, the rhombic splitting, V/λ, tetragonality, Δ/λ, and rhombicity, V/Δ,[17,18] are indicative of a nearly pure (95−98%) $(d_{xy})^1$ character with little spin-orbit mixing with the d_{xz} and d_{yz} orbitals. It should be noted that the Taylor model as used here ignores electron delocalization and does not enforce normaliza-

(54) Jameson, G. B.; Ibers, J. A. *Inorg. Chem.* **1979**, *18*, 1200.
(55) Hanack. M.; Renz, G.; Strahle, J.; Schmid, S. *Chem. Ber.* **1988**, *121*, 1479.
(56) Hanack, M.; Renz, G.; Strahle, J.; Schmid, S. *J. Org. Chem.* **1991**, *56*, 3501.
(57) Hahn, F. E.; Tamm, M. *J. Chem. Soc., Chem. Commun.* **1995**, 569.
(58) Collins, T. J.; Fox, B. G.; Hu, S. G.; Kostka, K. L.; Münck, E.; Rickard, C. E. F.; Wright, L. J. *J. Am. Chem. Soc.* **1992**, *114*, 8724.
(59) Scheidt, W. R.; Haller, K. J.; Hatano, K. *J. Am. Chem. Soc.* **1980**, *102*, 3017.
(60) Scheidt, W. R.; Lee, Y. J.; Luangdilok, W.; Haller, K. J.; Anzai, K.; Hatano, K. *Inorg. Chem.* **1983**, *22*, 1516.
(61) Scheidt, W. R.; Hatano, K. *Acta Crystallogr., Sect. C* **1991**, *C47*, 2201.
(62) Schappacher, M.; Fischer, J.; Weiss, R. *Inorg. Chem.* **1989**, *28*, 389.
(63) Malatesta, L.; Bonati, F. In *Isocyanide Complexes of Metals*; Wiley-Interscience: London, 1969; p 25.
(64) Vogler, A.; Rethwisch, B.; Kunkely, H.; Huttermann, J. *Angew. Chem., Int. Ed. Engl.* **1978**, *17*, 952.

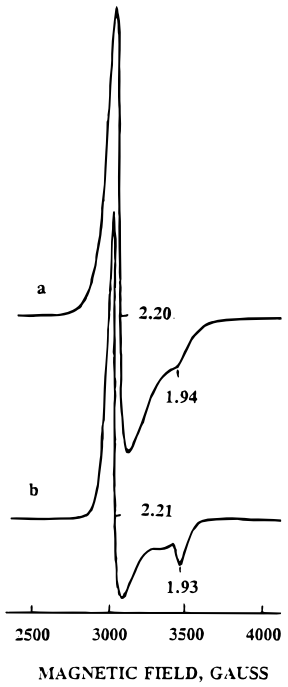

Figure 5. EPR spectra of [(TPP)Fe(*t*-BuNC)$_2$]ClO$_4$ (a) as the ground polycrystalline sample and (b) in a CH_2Cl_2 glass, both recorded at 77 K.

Table 3. Infrared and EPR Data for [(OEP)Fe(*t*-BuNC)$_2$]ClO$_4$ and [(TPP)Fe(*t*-BuNC)$_2$]ClO$_4$

	[(TPP)Fe(*t*-BuNC)$_2$]ClO$_4$	[(OEP)Fe(*t*-BuNC)$_2$]ClO$_4$
ν(NC), cm^{-1}	2200	2193
	Frozen CH_2Cl_2 Glassy EPR Spectra	
$g_\perp$	2.21	2.28
$g_\parallel$	1.93	1.83
$\sum g^2$	13.49	13.75
V/λ[a]	0.00	0.00
Δ/λ[a]	−8.33	−5.47
V/Δ[a]	0.00	0.00
%d$_{xy}$	98%	95%

[a] Calculated assuming Taylor's "proper axis system", with $g_y = -g_x = g_\perp$ and $g_z = -g_\parallel$.[18]

tion of the unpaired electron wave function. We have explicitly chosen the *z* direction to be the heme normal and $g_\parallel$ of the axial EPR spectrum to be g_z for the Taylor model (see footnote, Table 3). This is consistent with the effective geometric axial symmetry and all other physical measurements.

For these "purest" $(d_{xy})^1$ electronic ground states of Fe(III) porphyrinates found thus far, the *g*-values lead to a $\sum g^2 = 13.49-13.75$, $\Delta/\lambda = -8.3$ to -5.5 (the negative sign indicates that d_{xz} and d_{yz} are lower in energy than d_{xy}) and an average *g*-value of 2.12−2.14. Thus, a considerable amount (compared to [(TPP)Fe(4-CNPy)$_2$]ClO$_4$, where $\sum g^2 = 14.76$ and $\langle g \rangle = 2.22$[13]) of orbital angular momentum is quenched in these complexes, yet the *g*-values clearly identify the unpaired electron as predominantly occupying a metal d rather than a porphyrinate π molecular orbital composed of C and N p_z orbitals. (However, ^{1}H NMR results discussed below indicate that the porphyrinate character is large (∼19%).) The difference in *g*-values in this case still corresponds to a magnetic field difference $H_\parallel - H_\perp = 380-540$ G, which is *much* larger than that observed for the bis(*t*-BuNC) complex of the reduced heme (octaethylisobacteriochlorin) complex, (OEiBC)Fe(III) (∼40 G),[42] or for anion radical complexes of Ni(II) porphyrins or chlorins (<20 G).[65] (The latter have a different electronic ground state, $(4e_g(\pi^*))^1$, than that of interest here, but are probably representative of the possible degree of splitting of $g_\perp$ and $g_\parallel$ of a carbon-based radical center; few *low-temperature* EPR spectra of $(3a_{2u})^1$ ground-state cation radical centers have been reported thus far.) Therefore, it is not yet clear whether there is a smooth transition from the $(d_{xy})^1$ ground state, with small contributions from spin-orbit coupling, to the $(3a_{2u})^1$ ground state, or whether these two cases can clearly be distinguished on the basis of a significant difference in $g_\perp$ and $g_\parallel$ values alone. We have found, however, that almost identical EPR parameters are observed for the bis-*N*-methylimidazole complex of bis(dimethylglyoximato)iron-(III) ($g_\perp = 2.256$, $g_\parallel = 1.950$),[66] suggesting that these *could be* the limiting *g*-values for a "pure" $(d_{xy})^1$ ground state. For reasonable values of Δ/λ of −6 to −10 or even −15, the *smallest* possible $g_\perp - g_\parallel$ value is 0.15, corresponding to a peak separation, $\Delta H = H_\parallel - H_\perp$ of about 230 G at X-band (even for an unreasonably large $\Delta/\lambda = -20$, $\Delta H = 170$ G), and so the "gap" between this point and the <20 G peak separations of simple porphyrin radicals[65] would have to be filled by systems in which there is complete delocalization between metal d_{xy} and porphyrin p_z orbitals. Thus, the 40 G separation of [OEiBC)-Fe(*t*-BuNC)$_2$]$^{+}$ [42] remains intriguing and in need of further characterization, and other systems which may allow narrowing this gap should be sought.

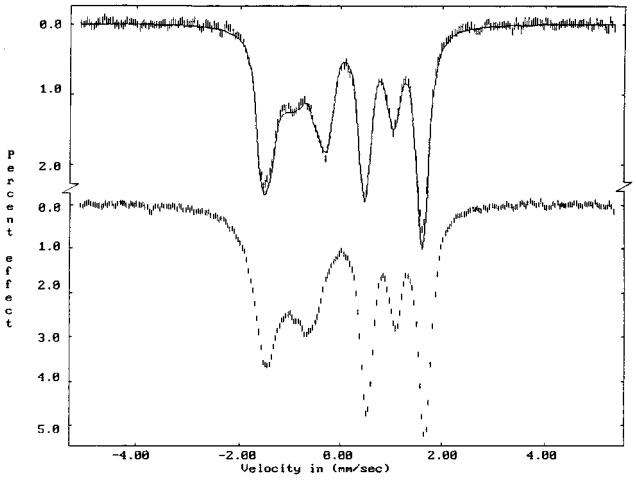

Figure 6. Mössbauer spectra of polycrystalline [(OEP)Fe(*t*-BuNC)$_2$]-ClO$_4$ (upper trace) and [(TPP)Fe(*t*-BuNC)$_2$]ClO$_4$ (lower trace) at 150 K in a 4.6 T field parallel to the γ beam. The solid line is a simulation based on a spin Hamiltonian in the fast fluctuation limit with the parameters listed in Table 4.

Mössbauer Spectra of the Bis(isocyanide) Complexes. The Mössbauer specta of the two bis(isocyanide) complexes, in pure form, displayed a single quadrupole doublet that was magnetically broadened even at ambient temperatures, the left line being broader than the right. The quadrupole splitting decreased slightly with increasing temperature, in the case of [(OEP)Fe-(*t*-BuNC)$_2$ClO$_4$ from ΔE_Q ∼2.06 mm/s at 4.2 K to ∼1.67 mm/s at 300 K. Polycrystalline samples showed further magnetic broadening in a 200 mT field at 4.2 K, but under these conditions the magnetic hyperfine interaction was largely averaged out by spin fluctuations.

In strong fields the doublets were observed to split in the manner expected for a negative quadrupole interaction, $V_{zz} < 0$, and small asymmetry parameter $\eta = (V_{xx} - V_{yy})/V_{zz}$, as illustrated in Figure 6. The temperature dependence of the splittings at constant field, moreover, allowed us to draw conclusions about the sign and approximate symmetry of the

(65) Fajer, J., personal communication.

(66) Young, D. M. and Walker, F. A., unpublished results.

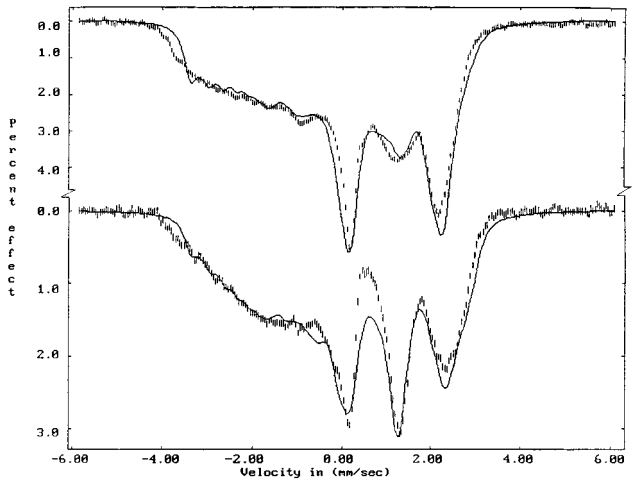

Figure 7. Mössbauer spectra of $[(OEP)^{57}Fe(t\text{-}BuNC)_2]ClO_4$ in frozen chlorobenzene solution at 4.2 K in a 220 mT field parallel (top) and perpendicular (bottom) to the γ beam. An extraneous line at 0.31 mm/s was subtracted as discussed in the text. The solid lines are simulations based on a spin Hamiltonian in the static limit with the parameters listed in Table 4.

internal field and hence the magnetic hyperfine interaction. The last step of this argument rests on the approximate isotropy of g^2. To be specific, for negative V_{zz} the left line of the quadrupole doublet arises from the $|1/2,\pm1/2\rangle$ to $|3/2,\pm3/2\rangle$ nuclear transitions, and since the splitting of this feature was observed to increase with temperature at constant field, the internal field and hence the product g_zA_z must be negative. The right (higher energy) line of the quadrupole doublet, on the other hand, arises from the $|1/2,\pm1/2\rangle$ to $|3/2,\pm1/2\rangle$ nuclear transitions, and since the splitting of this feature was observed to decrease with increasing temperature at constant field, one concludes that the product $g_\perp A_\perp$ must be positive. The simulation shown as solid line in the upper part of Figure 6 bears out these qualitative conclusions. It should be noted that the simulation assumes the limit of fast spin fluctuation rates and that the right feature approximates this limit more closely than the left one. For the TPP derivative (lower trace of Figure 6), no simulation is shown since the left feature is far from the fast fluctuation limit.

In order to resolve magnetic hyperfine interaction in the opposite limit of slow spin fluctuation rates we studied chlorobenzene solutions of ^{57}Fe-enriched TPP and OEP bis(isocyanides). Figure 7 shows 4.2 K spectra of $[(OEP)^{57}Fe(t\text{-}BuNC)_2]ClO_4$ in fields of 220 mT. Practically identical spectra were observed up to 15 K, indicating that a static spin Hamiltonian applies at these temperatures. Spectral simulations based on such a model are indicated by the solid lines in Figure 7. They match the spectral shapes reasonably well and reproduce, in particular, the dependence of the slope on the direction of the field. The hyperfine parameters deduced from the simulations are listed in Table 4; their discussion will be combined with that of the related parameters of the TPP derivative discussed below. It should be noted that the spectra of Figure 7 have been corrected for the presence of an extraneous line and may contain residual correction artifacts. The ^{57}Fe-enriched solution sample of $[(OEP)Fe(t\text{-}BuNC)_2]ClO_4$ actually contained a single-line impurity at $\delta = 0.31$ mm/s, which had also been encountered in earlier polycrystalline preparations. Since this extraneous line, which accounted for only 20% of the spectral area, had a peak absorption of about 5% on the scale of Figure 7 and evidently was not affected by the magnetic field, we have subtracted it for clarity in both traces of Figure 7.

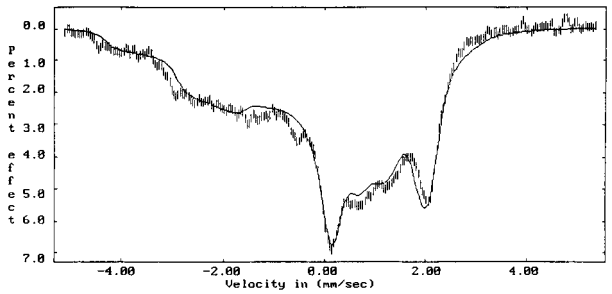

Figure 8. Mössbauer spectrum of $[(TPP)^{57}Fe(t\text{-}BuNC)_2]ClO_4$ in frozen chlorobenzene solution at 25 K in a 4.3 T field parallel to the γ beam. The solid line is a simulation based on a spin Hamiltonian in the limit of slow spin fluctuations with the parameters listed in Table 4.

Table 4. Mössbauer Parameters of $[(OEP)Fe(t\text{-}BuNC)_2]ClO_4$ and $[(TPP)Fe(t\text{-}BuNC)_2]ClO_4$

	OEP		
	polycrystalline (150 K)	solution (4.2 K)	TPP solution (4.2 K)
ΔE_Q[a] (mm/s)	−1.93	−1.80	−1.89
η	0.41	−0.14	0.09
Γ (mm/s)	0.23	0.31	0.36
$A/(g_N\beta_N)$ (T)	(20.6, 13.4, −23.4)	(18.8, 12.2, −36.3)	(8.7, 2.3, −34.2)
α, β, γ[b] (deg)	(0, 41, 0)	(9, 18, 0)	(0, 14, 0)

[a] ΔE_Q is given the sign of $V_{\zeta\zeta}$ or the quadrupole tensor component of largest magnitude. [b] Euler angles that describe the rotation from the principal axes of g and A to the axes of the quadrupole tensor.

Figure 8 shows a frozen chlorobenzene solution spectrum of $[(TPP)^{57}Fe(t\text{-}BuNC)_2]ClO_4$ in a 4.33 T field at 25 K with a superimposed spin Hamiltonian simulation in the limit of slow spin fluctuation rates. The parameters deduced from the simulation are listed with those of the OEP derivative in Table 4. Strong fields allow one to differentiate between positive and negative hyperfine couplings A_i or, more correctly, products of effective g- and A-tensors, g_iA_i. As can be seen in the table, both bis(isocyanide) complexes have identical signs and comparable magnitudes for corresponding components of the magnetic and the electric quadrupole tensors. No striking differences between crystalline and solution samples are noticeable either, apart from the different rates of spin fluctuations, of course. Obviously, the electronic structure of the iron must be nearly the same in the two compounds.

A comparison of the parameter sets in Table 4 reveals striking similarities in the hyperfine interactions of the two bis(isocyanide) complexes. The magnetic as well as the electric quadrupole interaction have roughly axial symmetry around z, the direction of the smallest component of the g-tensor, which can be assumed to coincide with the heme normal. The product g_zA_z is negative, while both perpendicular components are positive, as was already argued qualitatively in connection with Figure 6, based on the temperature dependence of the high-field spectra. The quadrupole interactions show a related pattern of approximate axial symmetry. The asymmetry parameters η are small, and the components of largest magnitude are negative, suggesting extra electron density along the approximate symmetry axis or less electron density in the perpendicular plane. While a small rotation of the quadrupole tensors by Euler angles α and β relative to the axes of the magnetic tensors improved the simulations, the main features of the spectra could be reproduced with coaxial tensors as well. By and large, therefore, in the bis(isocyanide) complexes the heme normal appears to be the symmetry axis of the quadrupole tensor as well as of the magnetic tensors. Moreover, the suggested lower electron density in the heme plane is consistent with a d_{xy} hole, the

electron configuration already proposed on the basis of the unusual *g*-values and the pattern of proton NMR shifts discussed below.

The signs and magnitudes of the magnetic hyperfine components, finally, are compatible with a d_{xy} hole as well. Given the wave functions of the t_{2g} hole as deduced from Taylor's model,[18] one can calculate the *A*-tensors according to Lang.[67] Since orbital reduction was ignored in Taylor's model, we set $k = 1$ as well, and we adopt the value $\kappa = 0.35$, where κ scales the isotropic Fermi contact term of the magnetic hyperfine tensor relative to the orbital and spin dipolar terms. The result is $A/(g_N\beta_N) = P[-0.234, 0.234, 0.752]$ for the OEP and $A/(g_N\beta_N) = P[-0.132, 0.132, 0.812]$ for the TPP derivative. Here, *P* is an overall scale factor, which assumes a maximum value of $P = 64$ T. Comparing these predictions with the empirical *A*-values of Table 4, it is clear that they match the symmetry but not the magnitude as long as *P* is kept at its maximum. Since *P* is proportional to $\langle r^{-3}\rangle$ of the unpaired electron and therefore decreases as the spin is delocalized, it is fair to treat it as a scale factor that can be adjusted to match the data. The best match (−12.0, 12.0, 38.5)T for OEP and (−5.6, 5.6, 34.2)T for TPP requires reductions in *P* from its maximum by 20% and 34%, respectively, implying very large spin delocalization in the TPP derivative.

An analogous approach predicts a valence contribution to the electric quadrupole splitting of $\Delta E_Q = -2.83$ mm/s for OEP and −2.93 mm/s for TPP, respectively, with $\eta = 0$ in both cases. Here, it has been assumed that a single 3d electron in a pure crystal field eigenstate produces a splitting of $\Delta E_Q = 3$ mm/s. Again, the prediction has the correct symmetry but too large a magnitude. The discrepancy in scale can be blamed on delocalization as an analogous factor $\langle r^{-3}\rangle$ controls the scale of the valence contribution, but here the average includes all 3d electrons. The most plausible explanation is full occupancy of the d_{xz} and d_{yz} orbitals and roughly $^4/_3$ of an electron in d_{xy} as a result of π donation from the porphyrin $3a_{2u}$ orbital. Such an explanation matches the 34% reduction of the magnetic hyperfine coupling in the TPP derivative noted above as well as the large spin density observed in the $3a_{2u}$ orbital from proton NMR studies of the OEP complex discussed below.

Thus, Mössbauer spectroscopy can clearly differentiate between these two possible electron configurations as well as between the $(d_{xz},d_{yz})^4(d_{xy})^1$ and $(d_{xy})^2(d_{xz},d_{yz})^3$ ground states. For systems having the latter pure electronic ground states, ΔE_Q is large ($\Delta E_Q = +2.28$ mm/s for $[(TMP)Fe(N\text{-}MeIm)_2]ClO_4$[6]), while for systems having somewhat "mixed" ground states, ΔE_Q is small ($\Delta E_Q = 0.65$ mm/s for $[(TPP)Fe(4\text{-}CNPy)_2]ClO_4$[13]), and ΔE_Q is again large (and negative) ($\Delta E_Q = -1.89$ mm/s for $[(TPP)Fe(t\text{-}BuNC)_2]\text{-}ClO_4$ (this work)) for cases in which the ground state is fairly pure $(d_{xz},d_{yz})^4(d_{xy})^1$. Thus magnetic Mössbauer spectroscopy, in which not only the size but also the sign of the quadrupole splitting is determined, is one of the most sensitive techniques for determining the nature of the electronic ground state of low-spin Fe(III) complexes.

^{1}H NMR Spectra. Proton NMR spectra of $[(TPP)Fe(t\text{-}BuNC)_2]ClO_4$ in CD_2Cl_2 as a function of temperature have been reported previously[14] and were the catalyst for the investigations reported herein. In this work we have investigated the proton NMR spectrum of $[(OEP)Fe(t\text{-}BuNC)_2]ClO_4$ in CD_2Cl_2 over a wide temperature range. Example spectra at 293 and 193 K are shown in Figure 9, and a Curie plot of the data obtained over the temperature range 173−310 K is shown in Figure 10. As can be seen in both Figures 7 and 8, the *meso*-H resonance is strongly shifted to negative ppm values, indicating very large

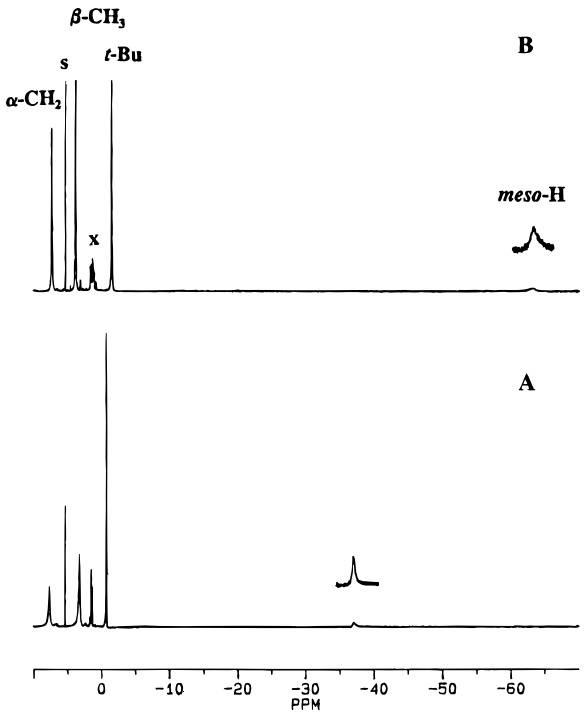

Figure 9. ^{1}H NMR spectra of $[(OEP)Fe(t\text{-}BuNC)_2]ClO_4$ in CD_2Cl_2 recorded at (a) 303 K and (b) 195 K. Assignments of the resonances are given in (b).

delocalization of the unpaired electron into π-symmetry orbitals of the porphyrinate ring having large electron density at the *meso*-carbon positions but very small electron density at the β-pyrrole carbon positions.[68,69] The Curie plot, while apparently linear for each type of proton, does not extrapolate to zero at infinite temperature for either the α-CH_2 or *meso*-H groups of the OEP ligand, as shown in the dashed lines of Figure 10. These two positions of the porphyrinate ring, the β-pyrrole and *meso*-carbon positions, are extremely sensitive to the expected electron density distribution in the filled porphyrinate π orbital involved in spin delocalization by porphyrin → Fe π donation.[68,69] While the $3e_g(\pi)$ orbitals have nodes at the *meso* positions and fairly large electron density at the β-pyrrole positions, only the $3a_{2u}(\pi)$ orbital has essentially zero electron density at the β-pyrrole but very large electron density at the *meso*-carbon positions.[70] The large *meso*-H contact shift[71] observed for this complex is about 19% that which can be calculated for the *meso*-H of a full $3a_{2u}(\pi)$ π cation radical species, based upon the EPR data obtained for $[Zn(Me)_4P]^{\bullet+}$.[72] While this comparison may not be quantitatively meaningful because of the probable large difference in core conformations of these two porphyrinates, it certainly indicates considerable spin delocalization to the $3a_{2u}(\pi)$ orbital of $[(OEP)Fe(t\text{-}BuNC)_2]ClO_4$. Thus, the large *meso*-H shifts observed (Figures 9 and 10) are extremely strong evidence for major spin delocalization from the d_{xy} orbital of the metal to the $3a_{2u}(\pi)$ orbital of the porphyrinate ring by porphyrin → Fe π donation, which is only possible if there is marked ruffling of the porphyrinate ring, such that the p_z orbitals of the

(67) Lang, G. *Quart. Rev. Biophys.* **1970**, *3*, 1.

(68) La Mar, G. N.; Walker, F. A. In *The Porphyrins*; Dolphin, D., Ed.; Academic Press: New York, 1979; Vol. IV, p 61.

(69) Walker, F. A.; Simonis, U. In *Biological Magnetic Resonance, Vol. 12: NMR of Paramagnetic Molecules*; Berliner, L. J., Reuben, J., Eds.; Plenum Press: New York, 1993; p 133.

(70) Longuet-Higgins, H. C.; Rector, C. W.; Platt, J. R. *J. Chem. Phys.* **1950**, *18*, 1174.

(71) −84.3 ppm, corrected for the calculated dipolar shift, based on the g-values of Table 2.

(72) Fajer, J.; Davis, M. S. In *The Porphyrins*; Dolphin, D., Ed.; Academic Press: New York, 1979; Vol. IV; p 201.

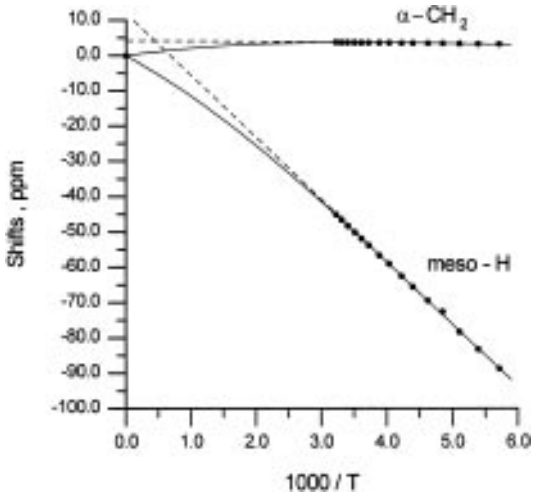

Figure 10. Curie plot of the *meso*-H and α-CH_2 resonances of [(OEP)-Fe(*t*-BuNC)$_2$]ClO_4. The dashed lines show the linear dependence, while the solid lines show the temperature dependence expected on the basis of a thermally-accessible excited state[73] with $\Delta E = 296$ cm^{-1}. The derived orbital coefficients for the ground and excited state orbitals are 0.0332 and 0.0084 for the *meso*-H, and −0.0004 and −0.0097 for the α-CH_2, respectively. The *meso*-H orbital coefficients are approximately one-quarter and twice those expected for the $3a_{2u}(\pi)$ and $3e_g(\pi)$ orbitals, respectively, on the basis of simple Hückel calculations,[70] although the exact size of the *meso*-H orbital coefficient is very dependent upon the energies of the d_π orbitals of the metal and thus the degree of mixing of $3e_g(\pi)$ and $4e_g(\pi^*)$ orbitals, which cannot be defined in this work. The α-CH_2 orbital coefficients are in the right relative size order for those expected for the β-pyrrole carbons for these two orbitals ($\rho_C = 0.004$ and 0.051, respectively). While the value of ΔE predicts a separation of ground and excited states much smaller ($\Delta E/\lambda = 0.74$ assuming $\lambda = 400$ cm^{-1}) than that expected from the value of $|\Delta/\lambda|$ determined from EPR spectroscopy (Table 3), the orbital coefficients of the excited state orbital are *not* consistent with involvement of $1a_{1u}(\pi)$, since that orbital has nodes at the *meso* positions.

porphyrinate nitrogens are significantly rotated from the normal to the mean plane of the porphyrin ring. This rotation of the p_z orbitals allows some fraction of p_z character to be mixed into the mean plane of the porphyrin ring, such that partial overlap with the d_{xy} orbital of the metal is possible. This same conclusion was reached for [(TPP)Fe(4-CNPy)$_2$]ClO_4, as shown in Figure 10 of ref SAFO ET AL, 1994, but the magnitude of the population of the $3a_{2u}(\pi)$ orbital was not estimated for that *meso*-phenyl complex. The considerable delocalization of the unpaired electron to the $3a_{2u}(\pi)$ orbital by π donation helps to explain the high degree of quenching of the orbital angular momentum that gives rise to a smaller $\langle g \rangle$ value for these bis-(isocyanide) complexes than has been reported for other iron-(III) porhyrinates having a predominantly $(d_{xy})^1$ ground state[7,13] and suggests that it may be possible to find other low-spin Fe-(III) complexes that will more closely approach the interface between the $(d_{xy})^1$ and $(a_{2u})^1$ ground states. It also helps to explain the required reduction in the Mössbauer scale factor, *P*, by 20% for this complex, as discussed above.

The nonzero intercepts of the Curie plot for the CH_2 and *meso*-H resonances (dashed lines shown in Figure 10) suggested that there might be a thermally-accessible excited state that affects the Curie dependence, as we have discussed recently.[73] (The temperature dependence of the quadrupole splitting noticed in the Mössbauer spectra may have the same origin.) A two-level fit of the NMR data according to eq 8 of ref 73 yields an energy separation of 295 cm^{-1} between the $(d_{xz},d_{yz})^4(d_{xy})^1$ ground state and its first excited state, which should have the configuration $(d_{xz},d_{yz})^3(d_{xy})^2$. The corresponding Curie plots are also shown in Figure 10 as the solid lines. It is interesting to note that although the energy separation between the ground state and the first excited state is only about 1.5 k_BT at room temperature, the NMR spectra are much more indicative of the $(d_{xy})^1$ ground state than are those of [(TPP)Fe(4-CNPy)$_2$]$^+$ [35] and [(TMP)Fe(4-CNPy)$_2$]$^+$ [7,74] where there is significantly less quenching of the orbital angular momentum. Comparison of the purest $(d_{xy})^1$ electronic ground state system, [(OEP)Fe(*t*-BuNC)$_2$]-ClO_4, to green heme systems that *could* have a $(d_{xy})^1$ ground state shows some striking differences. Licoccia *et al.* studied the NMR spectrum of the dicyanoiron(III) chlorin complex where the chlorin ligand was pyropheophorbide *a* methyl ester[40] and found that the pattern of isotropic shifts was most consistent with partial delocalization into the chlorin orbital analogous to the porphyrin $1a_{1u}(\pi)$ orbital. Significant in reaching this conclusion was the fact that the *meso*-H of the chlorin showed very small contact shifts.[40] The small *meso*-H shifts observed for the dicyanoiron(III) complex of pyropheophorbide *a* methyl ester are *not* consistent with major spin delocalization into the $3a_{2u}(\pi)$ orbital, in contrast to that for [(OEP)Fe(*t*-BuNC)$_2$]$^+$. It will be interesting to see whether this difference is due to the nature of the axial ligands or a combination of the axial ligands and the degree of reduction of the macrocycle. Studies of the *t*-BuNC complex of iron(III) pyropheophorbide *a* methyl ester are in progress in our laboratory.

Acknowledgment. The support of the National Institutes of Health, Grants DK-31038 (F.A.W.), GM-16406 (P.G.D.), GM-38401 (W.R.S.), and RR-06709 (W.R.S.) for X-ray instrumentation, and the University of Arizona Materials Characterization Program (F.A.W.) is gratefully acknowledged. The Department of Chemistry of the University of Arizona is grateful for support from the National Science Foundation, Grant DIR-9016385, for purchase of the EPR spectrometer. The authors wish to thank Dr. Tatjana Kh. Shokhireva for technical assistance.

Supporting Information Available: Tables S1−S12, complete crystallographic details, atomic coordinates, anisotropic thermal parameters, fixed hydrogen atom positions, bond distances and bond angles for [(TPP)Fe(*t*-BuNC)$_2$]ClO_4·0.75(C_6H_5Cl) and [(OEP)Fe(*t*-BuNC)$_2$]ClO_4 (23 pages.) See any current masthead page for ordering and Internet access instructions.

JA961971A

(73) Shokhirev, N. V.; Walker, F. A. *J. Phys. Chem.* **1995**, *99*, 17795.
(74) Watson, C. T.; Shokhirev, N. V.; Walker, F. A. To be submitted.